PHYSICAL REVIEW B **85**, 121304(R) (2012)

Spin-polarized states of matter on the surface of a three-dimensional topological insulator with implanted magnetic atoms

S. Caprara,[1,2] V. V. Tugushev,[1,3] P. M. Echenique,[1,4] and E. V. Chulkov[1,4]

[1]*Donostia International Physics Center (DIPC), P. de Manuel Lardizabal 4, 20018, San Sebastián, Basque Country, Spain*

[2]*Dipartimento di Fisica, Sapienza Università di Roma, Piazzale Aldo Moro 2, 00185 Rome, Italy*

[3]*RRC Kurchatov Institute, Kurchatov Square 1, 123182 Moscow, Russia*

[4]*Departamento de Física de Materiales, Facultad de Ciencias Químicas, Universidad del País Vasco (UPV)/Euskal Herriko Unibertsitatea (EHU) and Centro Mixto Consejo Superior de Investigaciones Científicas (CSIC-UPV/EHU), Apartado 1072, 20080 San Sebastián, Basque Country, Spain*

(Received 30 June 2011; revised manuscript received 12 January 2012; published 21 March 2012)

We describe the occurrence of a spin-polarized ferromagnetic state on the surface of a topological insulator with implanted 3*d* transition-metal atoms, within a model which takes into account the hybridization between the (s,p) orbitals of the insulator and the *d* orbitals of the metal, entailing the delocalized character of magnetic moments. Depending on the position of the Fermi level, the energy spectrum of this state displays both metallic and semimetallic, or semiconducting characteristics.

DOI: 10.1103/PhysRevB.85.121304 PACS number(s): 73.20.−r, 75.10.Lp

Three-dimensional topological insulators (TIs), such as the narrow-gap tetradymite semiconductors Bi_2Te_3 and Bi_2Se_3, have rather uncommon properties. Strong spin-orbit interaction not only affects the bulk electron spectrum of these materials, but also promotes peculiar surface states (SSs) with a conical (massless Dirac) spectrum,[1] which are weakly sensitive to Coulomb scattering on charged impurities, but are susceptible to exchange scattering on magnetic impurities. The effects of 3*d* transition-metal (TM) impurities (V, Mn, Fe, etc.) on the SSs of dilute magnetic semiconductors based on tetradymite TIs (e.g., $Bi_{2-x}Mn_xTe_3$ or $Bi_{2-x}Fe_xTe_3$) are particularly interesting,[2] since the implantation of magnetic atoms on the surface opens the way to a vast field of research aimed at combining the electronic properties of TIs with magnetic characteristics. For instance, chemisorption of Fe leads to a strong modification of the electron spectrum of the SSs on the (111) surface of Bi_2Se_3, and a gap $\Delta_g \approx 100$ meV appears with increasing Fe coverage ($>20\%$).[3] This result was explained in terms of ferromagnetic (FM) ordering of the local magnetic moments of Fe atoms in the direction orthogonal to the surface.

On the theoretical side, the effort to describe such an ordering was so far mainly devoted to obtain an effective interaction (mediated by the SS carriers of the TI) among the magnetic atoms, described as classical local moments (see, e.g., Ref. 4). If the chemical potential μ is finely tuned at the conical point of the spectrum of the SS, the effective interaction between two local moments at a distance r apart monotonically decays as r^{-3} and the magnetic phase diagram (Curie temperature versus concentration of magnetic moments) can be qualitatively obtained within a mean-field approach.[5] However, when μ falls within the band, a serious problem arises to identify the FM region in the phase diagram,[6] due to the appearance of an oscillating contribution to the interaction with slowly varying amplitude[7] ($\sim r^{-2}$) that makes the mean-field approach problematic. Recently,[8] a description was proposed, which treats the local moments at a mean-field level, in the case when these are localized in deep levels, but cannot describe the situation when the TM atoms form shallow levels near the conical point of the spectrum and are rather delocalized. Thus, the problem of the interaction among local moments on the surface of a TI calls for further investigation.

Our description of the SSs of a TI with implanted 3*d* TM magnetic atoms is based on the assumption that these atoms form shallow levels in a narrow-gap tetradymite semiconductor (possibly, with the exception of Mn, due to its rather small ionic radius). The 3*d* orbitals are then strongly hybridized with the (s,p) orbitals of the semiconductor, forming narrow (s,p)-*d* bands, the spins of the magnetic atoms are rather delocalized, and an itinerant description of magnetism is pertinent. Furthermore, the spectrum of the SS of a TI is robust against weak surface disorder, and the virtual crystal approximation for the surface is a good starting point to describe the spectrum of the system: The surface of a TI with implanted TM atoms is thereby described as a two-dimensional alloy forming an effective (average) crystal with lattice spacing a^*. In typical experimental conditions, due to chemical and technical limitations, the surface coverage is far from full, so that a^* may be larger than the typical lattice spacing a in the TI.

A further remark is in order. The *physical surface* of a TI comprises four or five layers, schematized in our description as a single ideal plane. Nonetheless, since magnetic atoms can be implanted on the topmost layer or *within* the physical surface, the hybridization between *d* and (s,p) orbitals may vary in experimental conditions. Our model is apt to capture the effect of this variation.

We describe the formation and FM ordering of local moments within an Anderson lattice model,[9] similar to the model for a magnetic δ layer in a semiconductor,[10] although important differences exist, the most remarkable being the absence here of band splitting in the spin-polarized state. We neglect the bulk electron states and consider only SSs extended along the surface and localized in the perpendicular direction. In a three-dimensional model, these states can be obtained in a way similar to that adopted to obtain Tamm SSs.[11]

Our model Hamiltonian is $\mathcal{H} = \sum_{\mathbf{p}} \mathcal{H}_{\mathbf{p}}$, with

$$\mathcal{H}_{\mathbf{p}} = \sum_{\alpha,\beta=\uparrow,\downarrow} v(\mathbf{p}\cdot\boldsymbol{\sigma})_{\alpha\beta}\, c^{+}_{\mathbf{p},\alpha} c_{\mathbf{p},\beta} + \sum_{\alpha=\uparrow,\downarrow} \varepsilon_{d,\alpha}\, d^{+}_{\mathbf{p},\alpha} d_{\mathbf{p},\alpha} + \sum_{\alpha=\uparrow,\downarrow} (V_{\mathbf{p}}\, c^{+}_{\mathbf{p},\alpha} d_{\mathbf{p},\alpha} + V^{*}_{\mathbf{p}} d^{+}_{\mathbf{p},\alpha} c_{\mathbf{p},\alpha}). \quad (1)$$

Here, v is the velocity of the (s,p) chiral particles at the surface of the TI, $\mathbf{p} \equiv (p_x, p_y)$ is a two-dimensional wave vector parallel to the surface, the operator $c^{(+)}_{\mathbf{p},\alpha}$ destroys (creates) an electron in the corresponding (s,p) state, with spin projection $\alpha = \uparrow,\downarrow$ onto the quantization axis, and $\boldsymbol{\sigma}$ is the vector of Pauli matrices. The d orbital level on the magnetic atom, $\varepsilon_{d,\alpha} = \varepsilon^{0}_{d} + U n_{d,-\alpha}$, includes a Hartree shift, resulting from the factorization of a Hubbard-like term $U n_{d,\uparrow} n_{d,\downarrow}$ which describes the correlated nature of the magnetic atom and promotes magnetism,[9] $n_{d,\alpha} = \langle N^{-1} \sum_{\mathbf{p}} d^{+}_{\mathbf{p},\alpha} d_{\mathbf{p},\alpha} \rangle$ is the average occupancy of electrons with spin projection α on the magnetic atom, N is the number of wave vectors $\mathbf{p}$ allowed by boundary conditions within the first Brillouin zone, and the operator $d^{(+)}_{\mathbf{p},\alpha}$ destroys (creates) an electron in the corresponding state. Finally, $V_{\mathbf{p}}$ is a (s,p)-d hybridization matrix element. We study the case of a single d orbital[10] and assume that the magnetic moments in the spin-polarized state are perpendicular to the surface. As TM atoms are rather far apart, we neglect the direct overlap of d orbitals.

The eigenvalues of the matrix

$$H_{\mathbf{p}} \equiv \begin{pmatrix} \varepsilon_{d,\uparrow} & 0 & V^{*}_{\mathbf{p}} & 0 \\ 0 & \varepsilon_{d,\downarrow} & 0 & V^{*}_{\mathbf{p}} \\ V_{\mathbf{p}} & 0 & 0 & vp^{*} \\ 0 & V_{\mathbf{p}} & vp & 0 \end{pmatrix},$$

where $p \equiv p_x + i p_y$ and $\sqrt{p^{*} p} = |\mathbf{p}|$, yield the spectrum of our model. A simple analytical expression is found in the nonmagnetic state. This is easily seen in the chiral basis,[12] where Eq. (1) reads

$$\mathcal{H}_{\mathbf{p}} = \sum_{\lambda=\pm} \lambda v |\mathbf{p}| c^{+}_{\mathbf{p},\lambda} c_{\mathbf{p},\lambda} + \sum_{\lambda,\nu=\pm} E_{d,\lambda\nu} d^{+}_{\mathbf{p},\lambda} d_{\mathbf{p},\nu} + \sum_{\lambda=\pm} (V_{\mathbf{p}}\, c^{+}_{\mathbf{p},\lambda} d_{\mathbf{p},\lambda} + V^{*}_{\mathbf{p}} d^{+}_{\mathbf{p},\lambda} c_{\mathbf{p},\lambda}), \quad (2)$$

with $E_{d,++} = E_{d,--} = \varepsilon_d \equiv \frac{1}{2}(\varepsilon_{d,\uparrow} + \varepsilon_{d,\downarrow})$, $E_{d,+-} = E^{*}_{d,-+} = -\Delta_p \equiv -\Delta e^{i\theta_p}$, where $\Delta \equiv \frac{1}{2}(\varepsilon_{d,\downarrow} - \varepsilon_{d,\uparrow}) = \frac{1}{2} U (n_{d,\uparrow} - n_{d,\downarrow})$ and θ_p is the phase of p. At $\Delta = 0$ the sub-blocks with $\lambda = \pm$ are evidently disjoint and the spectrum consists of two chiral bands,

$$\varepsilon^{\pm}_{\mathbf{p},\lambda} \equiv \tfrac{1}{2}[\varepsilon_d + \lambda v|\mathbf{p}| \pm \sqrt{(\varepsilon_d - \lambda v|\mathbf{p}|)^2 + 4|V_{\mathbf{p}}|^2}], \quad (3)$$

with $\lambda = \pm$. Henceforth, we take $V_{\mathbf{p}} \approx V_{\mathbf{p}=0} \equiv V$. The spectrum (3) has two conical points, at the energies $\varepsilon^{\pm}_{0} \equiv \frac{1}{2}(\varepsilon_d \pm \sqrt{\varepsilon_d^2 + 4|V|^2})$, with asymmetric velocities, $v_{\mp} \equiv \frac{1}{2}(1 \mp \varepsilon_d / \sqrt{\varepsilon_d^2 + 4|V|^2}) v$.

For $\Delta \neq 0$, the spectrum cannot be obtained analytically, but we can find the diagonal elements of the Green's function matrix $G(\zeta, \mathbf{p}) \equiv (\zeta I - H_{\mathbf{p}})^{-1}$, where ζ is a complex frequency, and I is the 4×4 identity matrix. We define the density of states (DOS) for real frequency ω,

$$\mathcal{N}_{r,\alpha}(\omega) \equiv -\frac{1}{\pi N} \sum_{\mathbf{p}} \mathrm{Im}\, G_{r,\alpha}(\zeta = \omega + i0^{+}, \mathbf{p}), \quad (4)$$

where $r = d,c$ labels the d and (s,p) diagonal components. Since $\mathrm{Im}\, G_{r,\alpha}$ depends on $\mathbf{p}$ only through $\varepsilon_{\mathbf{p}} \equiv v|\mathbf{p}|$, sums over $\mathbf{p}$ are transformed into energy integrals introducing the DOS for the spectrum $\varepsilon_{\mathbf{p}}$, $\mathcal{N}_0(\varepsilon) = |\varepsilon|/D^2$, for $|\varepsilon| \leqslant D$, and $\mathcal{N}_0(\varepsilon) = 0$, for $|\varepsilon| > D$, where the band half-width $D \equiv v\Lambda$ is taken henceforth as a reference energy unit, and the momentum cutoff $\Lambda \sim 1/a^{*}$ defines the Brillouin zone of the two-dimensional virtual crystal. Hereafter, we define $A_\alpha(\zeta) \equiv [\zeta B_{-\alpha}(\zeta) - |V|^2]/D^2$, $B_\alpha(\zeta) \equiv \zeta - \varepsilon_{d,\alpha}$. Then,

$$\int d\varepsilon\, \mathcal{N}_0(\varepsilon) G_{c,\alpha}(\zeta,\varepsilon) = \frac{A_\alpha(\zeta)}{B_{-\alpha}(\zeta)} \log \frac{\Phi(\zeta,0)}{\Phi(\zeta,D)},$$

where

$$\Phi(\zeta,z) \equiv B_\uparrow(\zeta) B_\downarrow(\zeta)(\zeta^2 - z^2) + \zeta |V|^2 [B_\uparrow(\zeta) + B_\downarrow(\zeta)] + |V|^4,$$

$$\int d\varepsilon\, \mathcal{N}_0(\varepsilon) G_{d,\alpha}(\zeta,\varepsilon) = \frac{1}{B_\alpha(\zeta)} \left[1 - \Upsilon_\alpha(\zeta) \log \frac{\Phi(\zeta,0)}{\Phi(\zeta,D)} \right],$$

with $\Upsilon_\alpha(\zeta) \equiv [|V|^4 - \zeta |V|^2 B_{-\alpha}(\zeta)]/[D^2 B_\uparrow(\zeta) B_\downarrow(\zeta)]$.

To obtain the phase diagram of the model, we solve two coupled self-consistency equations

$$n_{d,\alpha} = \int d\omega\, \mathcal{N}_{d,\alpha}(\omega) f(\omega - \mu) \quad (\alpha = \uparrow, \downarrow), \quad (5)$$

where $f(z) = [e^{z/T} + 1]^{-1}$ is the Fermi distribution function. Then, we calculate

$$n_{c,\alpha} = \int d\omega\, \mathcal{N}_{c,\alpha}(\omega) f(\omega - \mu) \quad (\alpha = \uparrow, \downarrow). \quad (6)$$

Here, we study the case when the chemical potential μ is fixed by the bulk, acting as a particle reservoir. Although real systems could be better described within an approach which is intermediate between fixing μ or the number of particles n, because of charge redistribution and screening effects, in Ref. 13 we showed that the two extreme descriptions, and a semiphenomenological intermediate description, yield similar results as far as the magnetic properties of a related model are concerned. The thermodynamical potential (per lattice site) is $\Omega = -T \int d\omega\, \mathcal{N}(\omega) \ln[1 + e^{(\mu-\omega)/T}] - U n_{d,\uparrow} n_{d,\downarrow}$, where $\mathcal{N}(\omega) = \sum_r \sum_\alpha \mathcal{N}_{r,\alpha}(\omega)$ is the total DOS, and the last term avoids double-counting of the Hartree energy.

The various phases are characterized by the partial magnetizations $m_r \equiv n_{r,\uparrow} - n_{r,\downarrow}$ $(r = d,c)$, obtained from the self-consistent solutions of Eqs. (5) and (6). In Fig. 1, we show a typical phase diagram in the U/D vs μ/D plane, at $T = 0$. In the absence of experimental or numerical indications, we adopted for the other parameters reasonable order-of-magnitude estimates $\varepsilon^{0}_{d}/D = -0.1$ and $|V|/D = 0.5$. The paramagnetic (PM) state, with the energy spectrum Eq. (3), is stable at U and/or μ smaller than some critical values, U_{cr} and μ_{cr}. At $U > U_{\mathrm{cr}}$ and $\mu > \mu_{\mathrm{cr}}$, a spin-polarized state occurs. The spins of the (s,p) electrons may be antiparallel or parallel to the spins of the d electrons, resulting in a ferrimagnetic (fm) or FM state, with $m_c m_d < 0$ (but $|m_c| < |m_d|$, so that

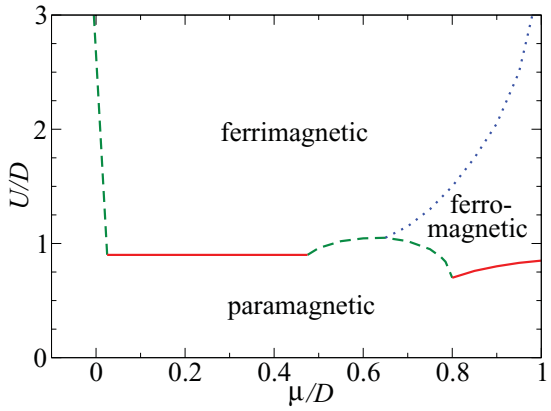

FIG. 1. (Color online) Phase diagram in the U/D vs μ/D plane at $T = 0$, for $\varepsilon_d^0/D = -0.1$ and $|V|/D = 0.5$. The solid (red online) and dashed (green online) lines mark second- and first-order phase transitions, respectively. The dotted (blue online) line separates the fm and FM states (see the text).

the magnetic moment is not compensated) or $m_c m_d > 0$, respectively. It must be borne in mind that the fm and FM states have the same symmetry and are not separated by a phase transition. The boundary between the two states is marked by the noncritical surface $m_c = 0$ in parameter space (dotted line). The transition between the PM and the spin-polarized (fm or FM) state can be first or second order (respectively, dashed and solid line). Increasing V has the effect of increasing both $U_{\rm cr}$ and (slightly) $\mu_{\rm cr}$, and pushes the fm-FM boundary line toward larger μ. The effect of changing ε_d^0 is altogether weak in a wide energy range but, as ε_d^0 approaches the conical point, the region of stability of the spin-polarized state is reduced.

The DOS of typical spectra is shown in Fig. 2. It is now clear that the nearly vertical first-order line at $\mu/D \approx 0$ and $U/D \gtrsim 0.9$ in Fig. 1 marks the transition from a PM metal [at $\mu/D \lesssim 0$, see Fig. 2(a)] to a fm semiconductor [at $\mu/D \gtrsim 0$, see Fig. 2(b)]. In the range $0 \lesssim \mu/D \lesssim 0.5$ and $U/D \gtrsim 0.9$ the chemical potential is located within a gap and the self-consistent solutions do not depend on μ/D (at $T = 0$). This is why the second-order line separating the PM and fm semiconducting phases in this range is a horizontal line at $U/D \approx 0.9$. At $\mu/D \gtrsim 0.5$ the fm state becomes metallic and the PM-fm transition becomes first order. Remarkably [see Fig. 2(c)], the fm state is characterized by a peculiar spectrum: The majority-spin DOS has a metallic character and is finite at the band edge, whereas the minority-spin DOS has a semimetallic character and vanishes linearly as the band edge is approached. This metallic-semimetallic state is reminiscent of the half-metallic state found in Ref. 10. Here, however, the band splitting in the spin-polarized state is not possible, because the chiral particles contribute to the spectral weight of both the majority- and minority-spin DOS. If μ is further increased, the fm metal is turned into a FM metal [see Fig. 2(d)], and eventually the PM-FM transition becomes second order, separating a PM metal and a FM metal.

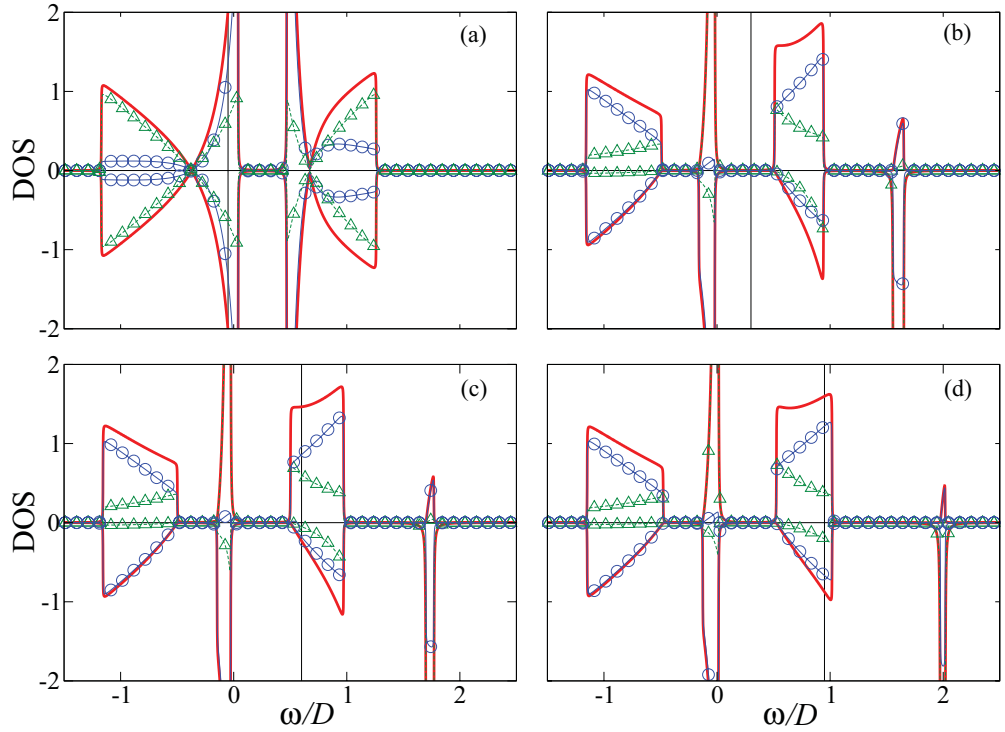

FIG. 2. (Color online) Majority- and minority-spin (plotted with a minus sign) DOS vs ω/D, for $T = 0$, $\varepsilon_d^0/D = -0.1$, $|V|/D = 0.5$, $U/D = 2.0$, and (a) $\mu/D = -0.05$ (PM metal), (b) $\mu/D = 0.3$ (fm semiconductor), (c) $\mu/D = 0.6$ (fm metal-semimetal), (d) $\mu/D = 0.95$ (FM metal). The vertical lines mark the position of the chemical potential. The solid (red online) lines mark the full DOS, and the open circles (blue online) and the triangles (green online) mark the (s, p) contribution [Eq. (4), with $r = c$] and the d contribution [Eq. (4), with $r = d$], respectively.

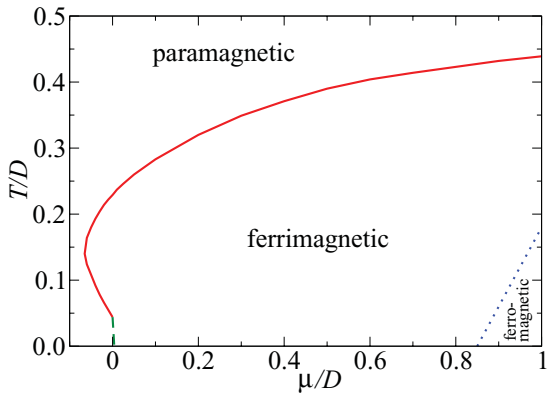

FIG. 3. (Color online) Phase diagram in the T/D vs μ/D plane, for $\varepsilon_d^0/D = -0.1$, $|V|/D = 0.5$, and $U/D = 2.0$. All lines have the same meaning as in Fig. 1.

Finally, we discuss the finite temperature phase diagram, reported in Fig. 3, for the same parameters as in Fig. 1 and $U/D = 2.0$. The first-order point at $\mu \approx 0$ and $T = 0$ evolves into a first-order line at $T \gtrsim 0$ (dashed line), which changes to second order when T is further increased (solid line). For $\mu \lesssim 0$, the fm state, unstable at $T = 0$, becomes stable in a finite temperature range. At $\mu > 0$, the fm phase evolves continuously to the PM phase with increasing T. The FM phase is always turned into the fm phase with increasing T (along the dotted line), which eventually undergoes a second-order transition to the PM phase with further increasing T.

Of course, the mean-field critical temperature obtained here must be interpreted as a temperature scale for the formation of local moments within the Anderson lattice model.[9] The true phase transition is ruled by thermodynamical fluctuations. In a genuinely two-dimensional spin-isotropic model, no transition exists at finite T. However, in real systems, relativistic and crystal-field effects introduce spin anisotropy of the easy-axis (Ising) or easy-plane (XY) type. In the case when the state with magnetization perpendicular to the surface is favored, the easy-axis anisotropy situation occurs, and the temperature for the two-dimensional Ising-like transition is fixed by the stiffness of transverse spin fluctuations[13] (fluctuation effects in related helical Fermi systems are also discussed, e.g., in Ref. 14).

Although we adopted an itinerant description of magnetism, some aspects of our results may be qualitatively compared with a result obtained within a localized description of the magnetic moments of the impurity atoms implanted on the surface of a TI. In Ref. 5, a phase diagram was drawn in the temperature versus spin anisotropy plane (in the case when the chemical potential is tuned at the conical point, to obtain a well-defined carrier-mediated exchange interaction), showing that the spin-polarized state exists at low temperature in the easy-axis and in the weakly easy-plane region. This state is the counterpart of the spin-polarized state found here, and could be recovered within our approach taking a deep d level ($|\varepsilon_d^0| \ll D$). The gap opening around the conical point in Ref. 5 has a counterpart in the gaps separating the two chiral bands of Fig. 2(a) in the spin-polarized state [see Figs. 2(b)–2(d)].

In conclusion, we have described the magnetic properties of the surface of a TI with implanted $3d$ TM atoms within an Anderson lattice model which accounts for the (s,p)-d hybridization and for the consequent delocalized character of the spin density. Within the mean-field approximation, which is well defined in our model even when μ is not finely tuned at the conical point of the spectrum of the TI, we have shown that the magnetic moments are ordered in a wide parameter range. The (s,p) and d contributions to the magnetization may be antiparallel or parallel, yielding a fm or FM state, respectively. The spectrum of the spin-polarized SSs has many intriguing properties: A fm semiconducting state or a fm state with metal-semimetal characteristics (for majority- and minority-spin carriers, respectively) occurs with varying the chemical potential. Our results call for further experimental and numerical (e.g., *ab initio*) investigations. For instance, we expect that light reflection experiments should detect the magneto-optic Kerr effect, and magnetotransport experiments should detect the anomalous contribution to the Hall effect, provided surface and bulk contributions are properly separated. The experiments of Ref. 3, on Fe-doped Bi_2Se_3, reveal the proliferation of conical points, as found in this Rapid Communication [see Fig. 2(a), with two conical points in our simplified description, lacking d orbital degeneracy], as well as the formation of subbands separated by gaps [see Figs. 2(b)–2(d)]. Recent *ab initio* calculations for the (111) surface of Mn-doped Bi_2Te_3 revealed a half-metallic spectrum,[15] which should compare to our spectrum of Fig. 2(c), where, however, a small but finite spectral weight of minority spins persists at the Fermi level.

The work was partially supported by the University of the Basque Country (Proyecto GV UPV/EHU Grant No. IT-366-07), Spanish Ministerio de Ciencia y Tecnologia (Grant No. FIS2010-19609-C02-01), and by RFBR (Grant No. 10-02-0018-a).

[1] L. Fu and C. L. Kane, Phys. Rev. B **76**, 045302 (2007); M. Z. Hasan and C. L. Kane, Rev. Mod. Phys. **82**, 3045 (2010); X.-L. Qi and S.-C. Zhang, *ibid.* **83**, (2011).

[2] V. A. Kulbachinskii, A. Yu. Kaminskii, K. Kindo, Y. Narumi, K. Suga, P. Lostak, and P. Svanda, Physica B **311**, 292 (2002); J. Choi, S. Choi, J. Choi, Y. Park, H.-M. Park, H.-W. Lee, B.-C. Woo, and S. Cho, Phys. Status Solidi B **241**, 1541 (2004); Y. S. Hor, P. Roushan, H. Beidenkopf, J. Seo, D. Qu, J. G. Checkelsky, L. A. Wray, D. Hsieh, Y. Xia, S.-Y. Xu, D. Qian, M. Z. Hasan, N. P. Ong, A. Yazdani, and R. J. Cava, Phys. Rev. B **81**, 195203 (2010).

[3] L. A. Wray, S.-Y. Xu, Y. Xia, D. Hsieh, A. V. Fedorov, Y. S. Hor, R. J. Cava, A. Bansil, H. Lin, and M. Z. Hasan, Nat. Phys. **7**, 32 (2011).

[4] Q. Liu, C.-X. Liu, C. Xu, X.-L. Qi, and S.-C. Zhang, Phys. Rev. Lett. **102**, 156603 (2009); F. Ye, G. H. Ding, H. Zhai, and Z. B. Su, Europhys. Lett. **90**, 47001 (2010); J.-J. Zhu, D.-X. Yao, S.-C. Zhang, and K. Chang, Phys. Rev. Lett. **106**, 097201 (2011).

[5] D. A. Abanin and D. A. Pesin, Phys. Rev. Lett. **106**, 136802 (2011).

[6] R. R. Biswas and A. V. Balatsky, Phys. Rev. B **81**, 233405 (2010).

[7]M.-T. Tran and K.-S. Kim, Phys. Rev. B **82**, 155142 (2010).
[8]V. N. Men'shov, V. V. Tugushev, and E. V. Chulkov, JETP Lett. **94**, 629 (2011).
[9]P. W. Anderson, Phys. Rev. **124**, 41 (1961).
[10]S. Caprara, V. V. Tugushev, P. M. Echenique, and E. V. Chulkov, Europhys. Lett. **85**, 27006 (2009).
[11]V. A. Volkov and T. N. Pinsker, Sov. Phys. Solid State **23**, 1022 (1981).
[12]X.-Y. Feng, W.-Q. Chen, J.-H. Gao, Q.-H. Wang, and F.-C. Zhang, Phys. Rev. B **81**, 235411 (2010); R. Žitko, *ibid.* **81**, 241414(R) (2010).
[13]S. Caprara, V. V. Tugushev, and E. V. Chulkov, Phys. Rev. B **84**, 085311 (2011).
[14]C. Xu, Phys. Rev. B **81**, 054403 (2010).
[15]C. Niu, Y. Dai, M. Guo, W. Wei, Y. Ma, and B. Huang, Appl. Phys. Lett. **98**, 252502 (2011).